Basic features of electromagnetic pulse generated in a laser-target chamber at 3-TW laser facility PALS

2014 J. Phys.: Conf. Ser. 508 012007

(http://iopscience.iop.org/1742-6596/508/1/012007)

Basic features of electromagnetic pulse generated in a laser-target chamber at 3-TW laser facility PALS

M De Marco[1], M Pfeifer[1], E Krousky[1], J Krasa[1], J Cikhardt[2], D Klir[2] and V Nassisi[3,4]

[1]Institute of Physics, ASCR, v.v.i., Na Slovance 2, 182 21 Praha 8, Czech Republic
[2] Czech Technical University, Technická 2, 166 27 Prague 6, Praha 6 Czech Republic
[3]LEAS, Dipartimento di Matematica e Fisica, Università del Salento
[4]INFN Sezione di Lecce, Via Arnesano, sn – 73100 Lecce, Italy

E-mail: demarco@fzu.cz

Abstract. We describe the radiofrequency emission taking place when 300 ps laser pulses irradiate various solid targets with an intensity of 10^{16} W/cm^2. The emission of intense electromagnetic pulses was observed outside the laser target chamber by two loop antennas up to 1 GHz. Electromagnetic pulses can be 800 MHz transients, which decay from a peak electromagnetic field of $E_0 \cong 7$ kV/m and $H_0 \cong 15$ A/m. The occurrence of these electromagnetic pulses is associated with generation of hard x-rays with photon energies extending beyond 1 MeV. This contribution reports the first observation of this effect at the PALS facility.

1. Introduction

If a high intensity laser pulse irradiates a target, the production of plasma can be accompanied by the emission of an intense electromagnetic pulse (EMP) within and outside the laser target chamber [1-10]. The EMP causes electromagnetic interference and can disrupt or damage nearby electronic diagnostics and control units. It is supposed that the EMP arises in the laser target chamber where the short-pulse laser produces energetic electrons that are able to escape the target until the built electrostatic field is low enough [3]. The short pulse of electrons can produce very high transient currents and intense EMP with broad spectrum ranging from several tens of MHz to several GHz. The occurrence of small-scale structures in a laser-target chamber contributes to the fraction of the EMP that is at higher frequencies [4]. Just for effective mitigation of diagnostic-generated electromagnetic interference it is essential to know the characteristics of the EMP. The interference between the EMP and ion collector (IC) signal can also be identified in Fig. 2 of [11] which were produced by a 500 ps laser pulse irradiating a target with intensity of ~10^{14} W/cm^2. The aim of the work reported here is to characterize the EMP, which has been produced by the laser facility PALS delivering intensity up to 3×10^{16} W/cm^2 onto a target in 300-ps pulses.

2. Experimental arrangement

The 3-TW PALS laser system irradiated 10 μm silicon and 200 μm plastics targets at 0° and 30° with respect to the target normal. The emission of ions was measured with the use of TOF ion collectors

and EMP was detected with the use of 12 cm diameter Moebius loop antennas [14]. Other devices used are TEKTRONIX DPO4104 2.5 GS/s 1 GHz oscilloscope and Rg-58 coaxial cables. Fig. 1 shows the scheme of the target chamber and the loop antenna. An ion ring collector IC with internal diameter of 3.8 cm and outer one of 5.0 cm was used to measure the ion component of the plasma expanding into the vacuum; the schematic drawing of the used collector is in [12].

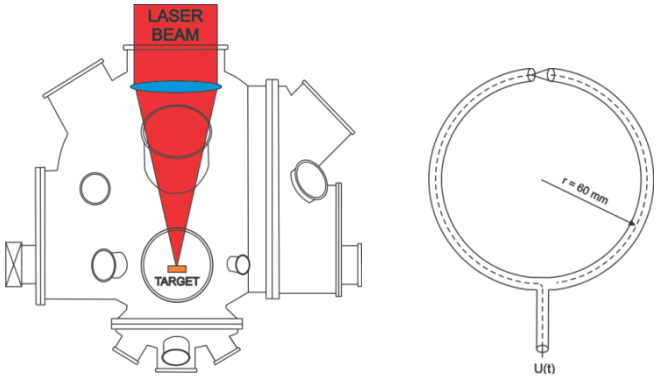

Figure 1. Schemes of the target chamber and the loop antenna.

3. Experimental results

Fig. 2a shows a typical example of a strongly degraded ion collector signal caused by the EMP interference. The observed EMP wavefront at ~12 ns prior the XUV-signal clearly reveals a propagation delay of the IC signal. This delay is proportional to the length of the used coaxial cable, as Fig. 2b shows. This experimental finding can be useful in some other experiments because this fact allows us to eliminate the EMP interference, e.g. by inserting a delay unit (e.g. a long Rg-58 coaxial cable) between the oscilloscope and IC, as it was proposed by one of our team (M.P.). The propagation delay of the IC signal passing through a 40-m coaxial cable on the interference is shown in Fig. 2b. It reveals that the EMP is not a part of the IC signal because it is not coupled to the active part of the TOF detector and, thus, it is not propagating with the signal induced by XUV radiation and ions. Nevertheless, the acceptable very low capturing of these fast transient events in the harsh electromagnetic environment occurring in the vicinity of the beam-target interaction chamber has been performed when the oscilloscope was protected inside a Faraday cage.

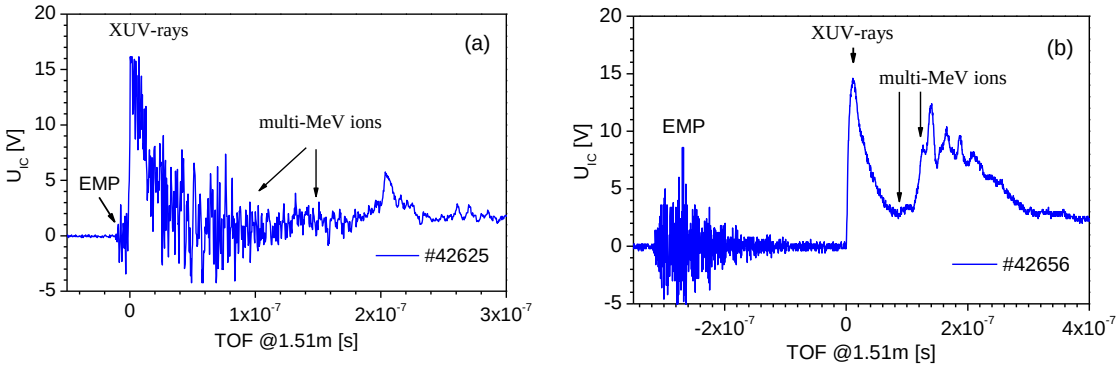

Figure 2. Interference between EMP and IC signal (a). Separation of the EMP from the IC signals inserting a delay unit between oscilloscope and IC (b). The $(CD_2)_n$ target was exposed to $I_L = 2\times10^{16}$ W/cm^2.

The transient signals in the vicinity of the target chamber were recorded using the Moebius loop antennas. All the EMP waveforms observed in the PALS experiment have a similar structure, as Fig. 3

shows; the antenna was placed vertically to the ground above the target chamber at a distance of 0.5 m. The analysis of the waveform based on a band pass FFT filter method shown that its first part lasting about 50 ns (labelled by ΔT_1 in Fig. 3) has a frequency spectrum ranging from ~370 MHz to ~ 610 MHz. The central part that is stronger (labelled by ΔT_2 in Fig. 3) has a frequency spectrum from ~690 MHz to ~ 850 MHz. Although the magnitude and frequency of the EMP generated within an ideal spherical, cylindrical or rectangular target chamber can be calculated, the behaviour of a real target chamber is different due to its shape (see Fig. 1) and the effect of equipment inside the chamber [1]. Such a target chamber has multiple, distinct, resonant frequencies which can only be determined experimentally.

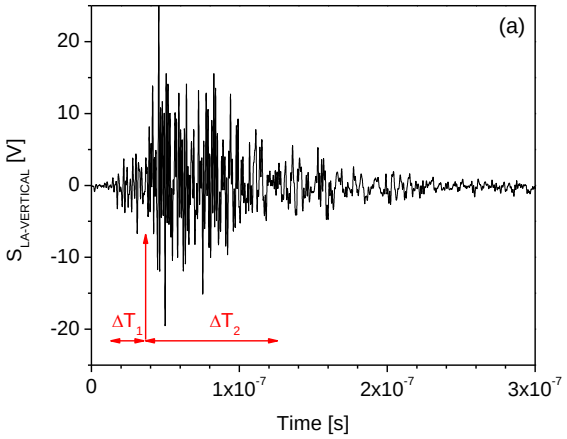

Figure 3. Example of vertical loop antenna waveform; the antenna was positioned above the laser target chamber at a distance of 0.5 m. A 10-μm thick Si single crystal foil was exposed to the laser intensity of 2×10^{16} W/cm^2.

The distribution of the electromagnetic field in the laboratory room has a complex structure mainly due to the different EMP spread through the wall and the windows of the laser target chamber, as Fig. 4 shows. The comparison of the FFT spectra clearly demonstrates that the glass window is quite more transparent for the EMP. Thus, if the detector is positioned near this window, than the induced noise signal can reach a high value and the detector signal is degraded. The measurements show that the signals passing through the glass windows are about three times higher than the signals passing through the steel wall.

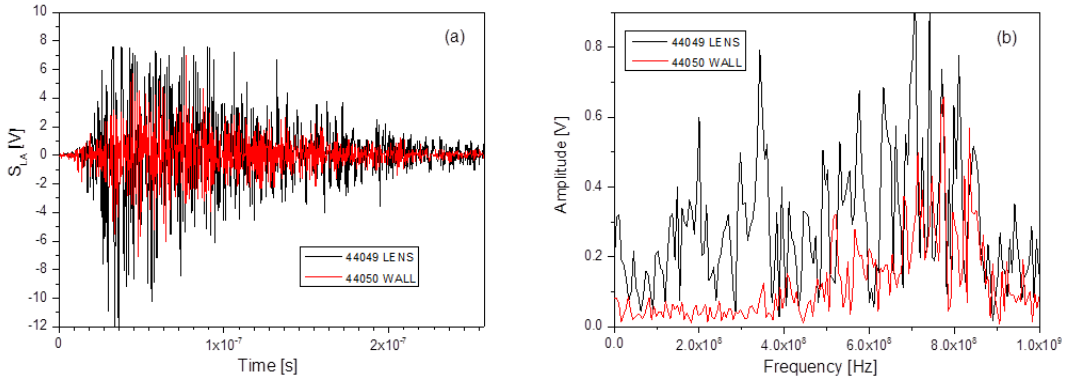

Figure 4. Loop antenna signals detected outside the target chamber beyond the laser-beam input glass window (near the focussing lens) and beyond the steel wall (a) and corresponding FFT spectra (b). A 10-μm thick Si single crystal foil was exposed to the laser intensity of 4×10^{16} W/cm^2.

From the experiment described in [15] we know that using the loop antenna positioned into the target chamber, the values of electric field inside the target chamber were determined to be in average

$E_0 \cong 7$ kV/m for $(CD_2)_n$ targets exposed to intensity of 10^{16} W/cm^2. The comparison of EMP signals detected at the same shot by the loop antenna placed inside the chamber (less or more in the middle of the chamber) [15] and by our loop antenna outside at 0.6 m behind the steel wall, shows that there is a wall attenuation of about 20 dB. Our measurements confirm the experiences with shielding and EMP mitigation strategy presented in [5,6] which is based on optimized grounding and detector configurations.

4. Conclusions

Our experiment has shown that the laser system PALS delivering onto a target the intensity of about 4×10^{16} W/cm^2 can generate not only protons up to 4-MeV [13] but also damaging intense EMP. The frequency spectrum of the detected EMP ranges up to 1GHz. As expected, also in the case of the PALS target chamber, the EMP behaviour is different from one in ideal spherical chamber. In fact due to the effects of small-scale structures in the target chamber as well as of equipment inside the chamber such as the target positioner, cameras, Faraday cups, and other detectors, there is a shift in the ideal spherical chamber resonant frequency [1]. Bunche structure of the generated EMP, where bunches have different mean frequencies and appear at different times, could be due to bursts of plasma escaping the target, and propagating through the target chamber and then interact with the target chamber wall. The most intense EMP outside the target chamber was observed near the large area glass window (corresponding attenuation is ~10dB).

A topic for future investigation will be using various solid target materials and novel plasma diagnostics allowing us e.g. measuring the target holder current and plasma expansion with the application of femtosecond interferometry.

Acknowledgements

The authors gratefully acknowledge the support of the staff of the PALS laser facility without whose assistance this work would not has been possible. The research leading to these results has received funding from the Czech Science Foundation (Grant Nos. P205/12/0454), the Czech Republic's Ministry of Education, Youth and Sports (grant for the PALS RI - Project IC: LM2010014, and for the OPVK 3: CZ.1.07/2.3.00/20.0279), and from the LASERLAB-EUROPE (grant agreement n° 284464, EC's Seventh Framework Programme).

References

[1] M. J. Mead, et al., *Rev. Sci. Instrum.* **75** (2004) 4225 - 4227.
[2] J. Raimbourg, *Rev. Sci. Instrum.* **75** (2004) 4234 - 4236.
[3] F. S. Felber, *Appl. Phys. Lett.* **86** (2005) 231501.
[4] C. Stoeckl, et al., *Rev. Sci. Instrum.* **77** (2006) 10F506.
[5] C. G. Brown Jr., et al., *J. Physics: Conf. Ser.* **112** (2008) 032025.
[6] D. C. Eder, et al., LDRD Final Report LLNL-TR-411183, LLNL, 2009.
[7] C. G. Brown, et al., *Rev. Sci. Instrum.* **83** (2012) 10D729.
[8] N. L. Kugland, et al., *Appl. Phys. Lett.* **101** (2012) 024102.
[9] A. L. Galkin, et al., *Contrib. Plasma Phys.* **53** (2013) 109 – 115.
[10] F. Consoli, et al., *Nucl. Instr. Meth. Phys. Res.* A **720** (2013) 149–152.
[11] E. Woryna, et al, *Appl. Phys. Lett.* **69** (1996) 1547-1549.
[12] E. Woryna et al. *Laser Part. Beams* **14** (1996) 293-321.
[13] J. Krasa, D. Margarone, *AIP Conf. Proc.* **1462** (2012) 139-142.
[14] C. E. Baum. Pulse Sensor Characteristics of the Moebius Strip Loop. Electromagnetic and Simulator Notes, Note 7, 1964. http://www.ece.unm.edu/summa/notes/Sensor.html.
[15] D. Kocon, et al. Proceedings of IBIC2013, Oxford, UK. MOPF05, pp 208-211.